The opportunities for laser-driven medicine at ELI-NP

Extreme Light's Modernistic Application
ELI-N
Magurele, Romania
July 7, 201

T. Tajima
Norman Rostoker Chair Professor, UC Irvine
Chair, International Comm Utrahigh Intensity Lasers
Chair, ELI-NP International Science Advisory Board

Acknowledgments for Collaboration: G. Mourou, J. A. Wheeler, X. M. Zhang, M. Zhou, S. Galles, D. Farinella, , K. Nakajima, V. Zamfir, Y.M. Shin, C. Barty, X. Q. Yan, P. Taborek, A. Bracco, F. Dollar, . Tromberg, D. Roa, C. Barty, F. Tamanoi, F. Dollar, T. Hayakawa, K. Nakajima, and ELI-NP staff

Recent breakthrough (as of 2009)

From **incoherent (or heating)** of electrons

to **Coherent drive of them**

↓

↓

CAIL (Coherent Acceleration of Ions by Laser)

TNSA (Target Normal Sheath Acceleration)

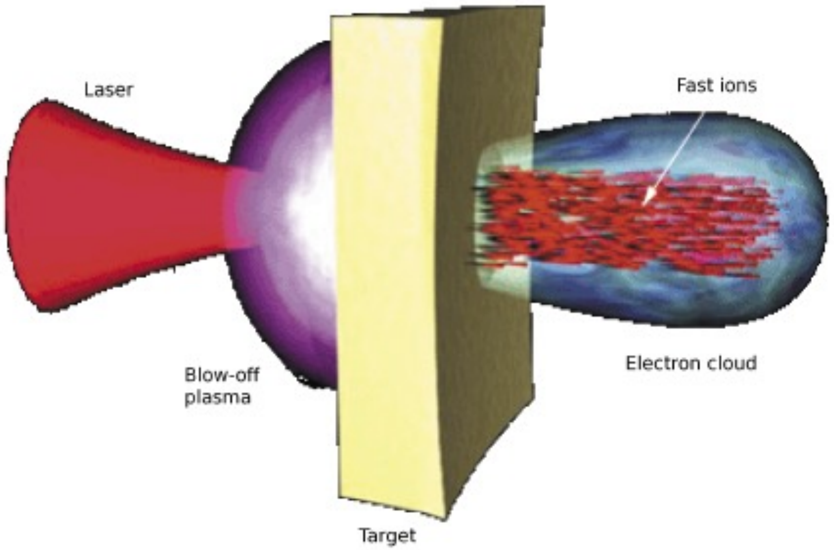

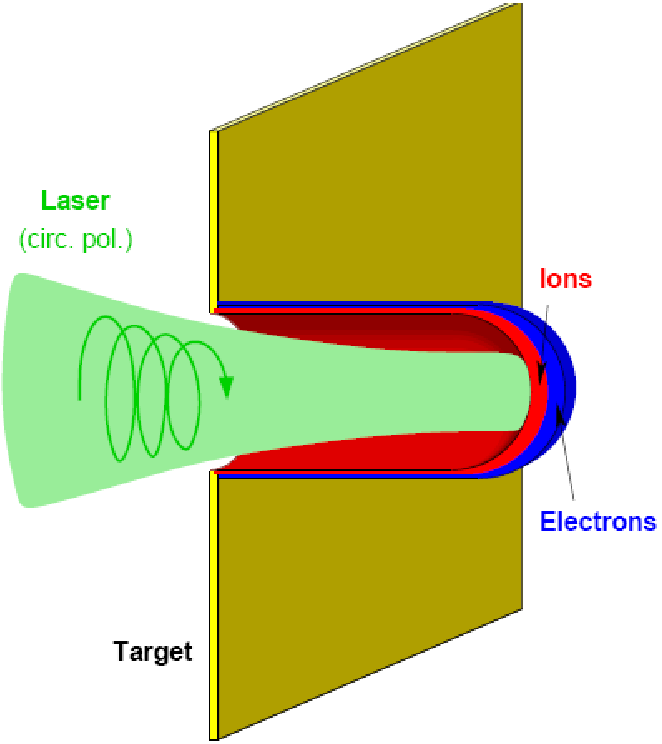

Experiments in CAIL Regime

Ultrathin film **:$\sigma = a_0$, where $\sigma = d\ n / \lambda n_c$ ($\xi=\sigma/a_0$)**
High laser contrast: not to destroy ultrathin target

ξ=1 ↓

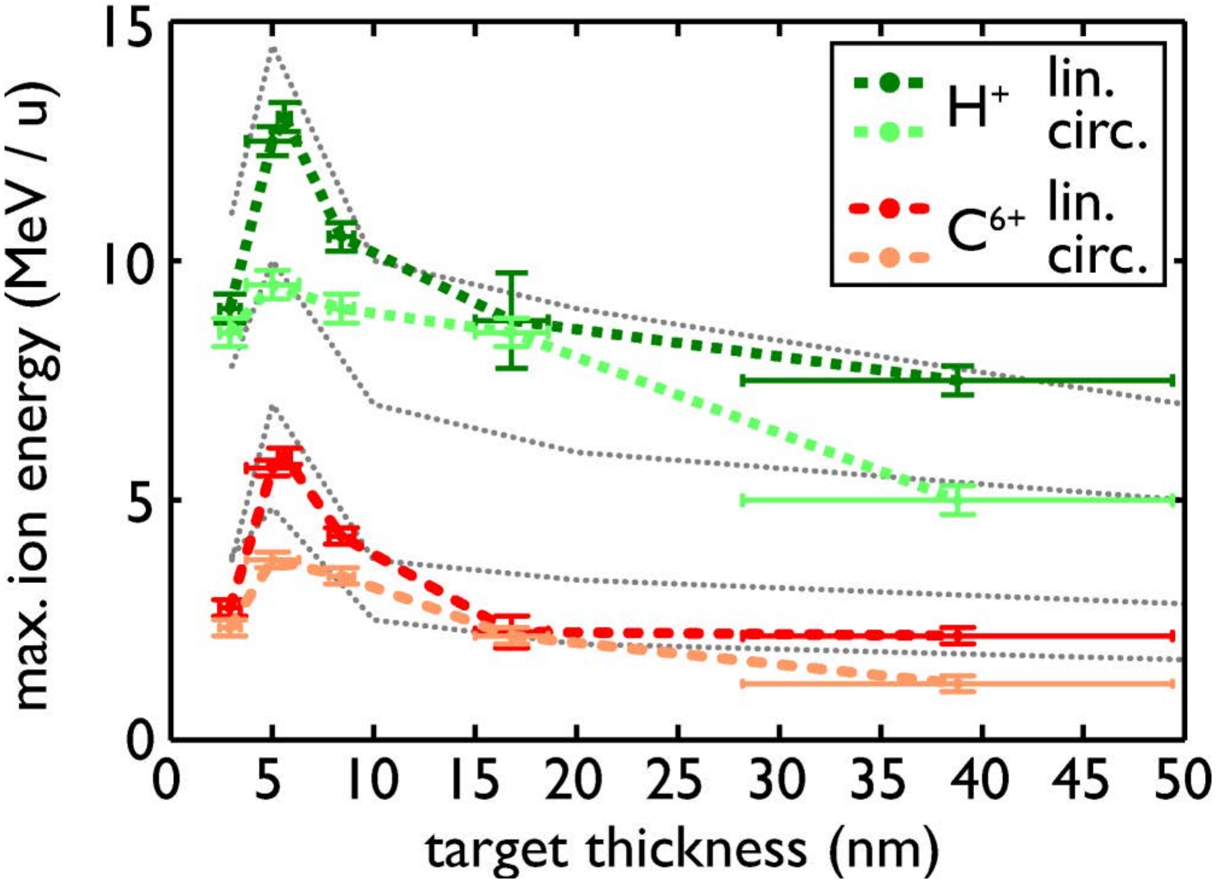

MAP + MBI

(Henig et al, 2009)

comparison of the phase space dynamics

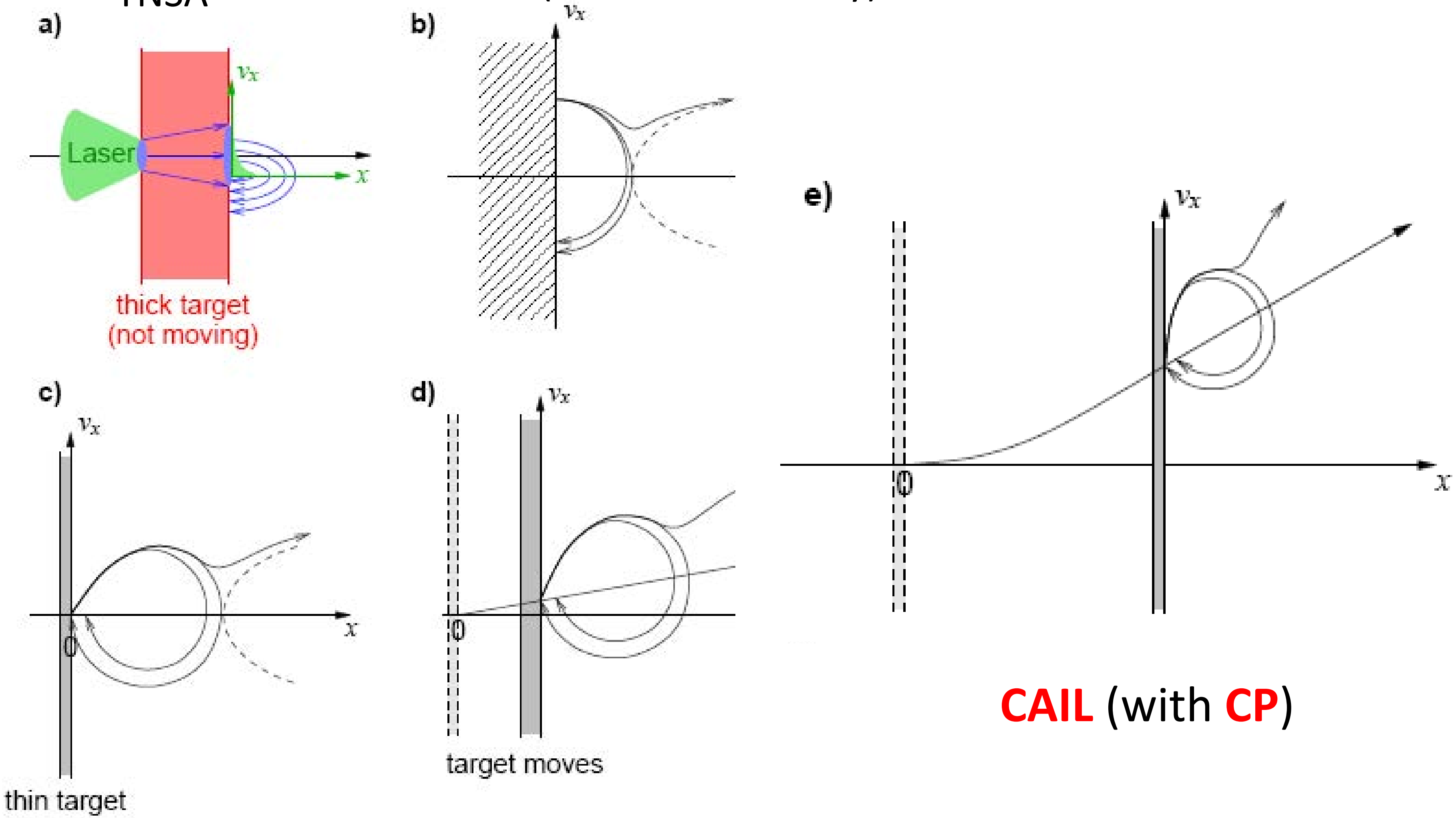

TNSA

(metallic boundary)

CAIL (with **CP**)

CAIL

Energy Gain in Laser Ion acceleration: CAIL (Coherent Acceleration of Ions by Laser) regime

- When electron dynamics by laser drive is sufficiently coherent, with coherence parameter α of electrons, the ion energy in terms of electron energy is :

$$\varepsilon_{\max,i} = (2\alpha + 1)\, Q\, \varepsilon_0$$

Ion energy

(*the more coherent the electron motion, the higher the ion energy*)

$$\varepsilon_0 = mc^2 \left(\sqrt{1 + a_0^2} - 1 \right)$$

Electron energy =
ponderomotive energy

$$\varepsilon_{\max,i} = (2\alpha + 1)\, Q \bar{\varepsilon}_0(t_1) \left((1 + \omega_L\, t_1)^{1/2\alpha+1} - 1 \right)$$

α maximizes at ξ = 1

Synchrotron oscillations in the bucket

Laser drives accelerating bucket,
more adiabatic trapping structure

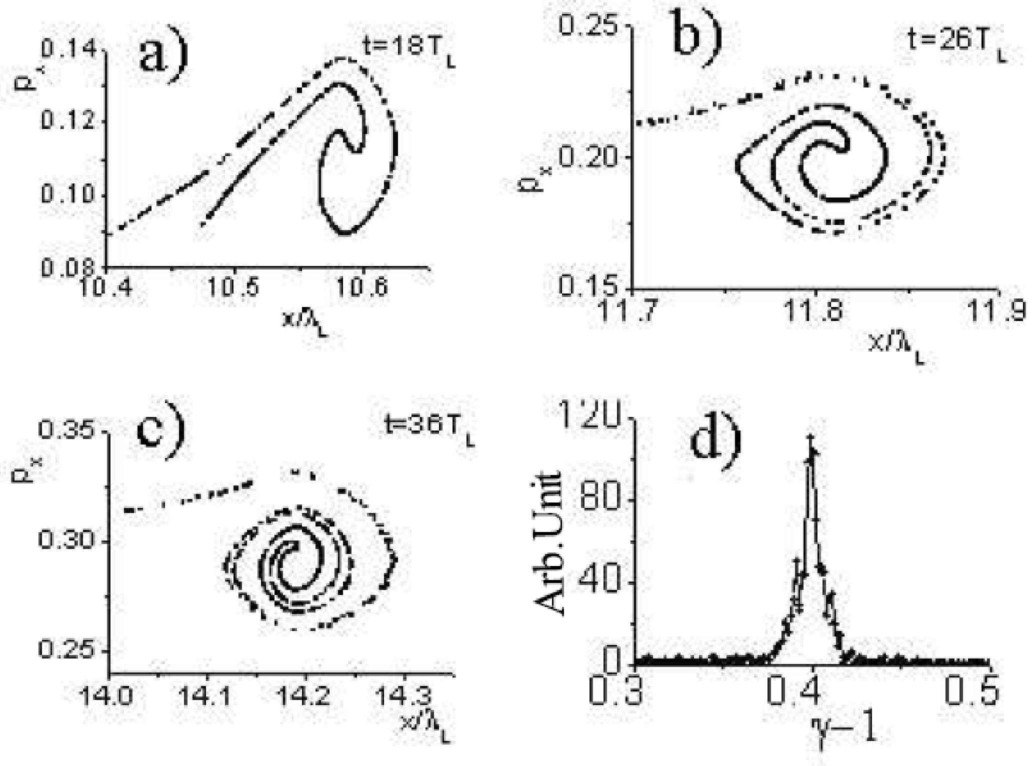

Monoenergy spectrum

(a,b,c)Evolution of phase space distribution for protons, the 1st, 2nd and 3rd oscillation period are 8, 8 and 10 T respectively. (d)Energy spectrum of protons.

Circularly polarized laser driven

CP laser drives ions out of ultrathin (nm) foil **adiabatically**
Monoenergy peak emerges

Bucket trapping ions
↓

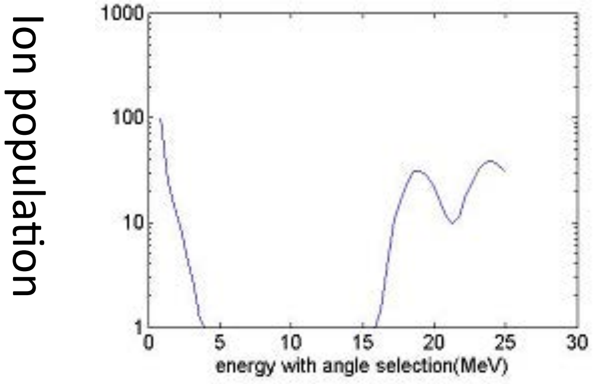

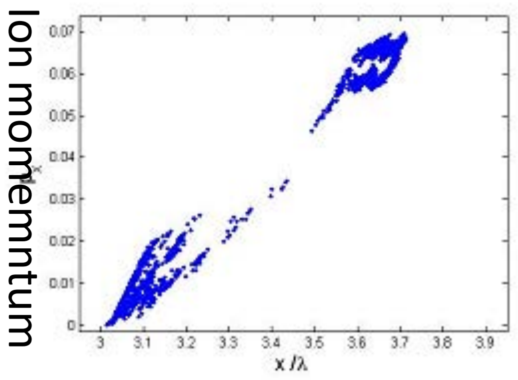

⇇ $V_{i,tr}$

laser →

→

$$V_{i,tr} = c\sqrt{(a_0 m/M)}$$

(X. Yan et al: 2009)

Ponderomotive force drives electrons,
Electrostatic force nearly cancels
Slowly accelerating bucket formed

Laser -Thin Foil Interaction

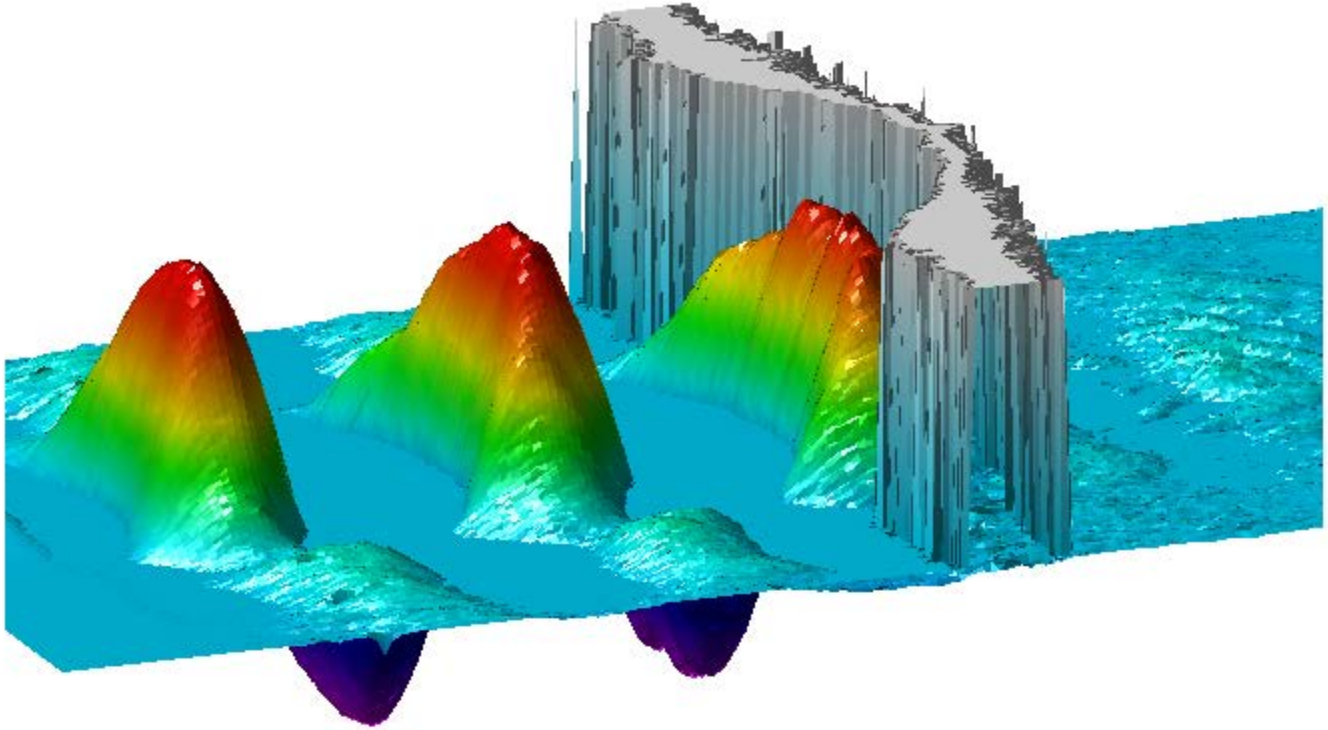

X. Yan, Habs, et al., 2009

Maximum energies of ions

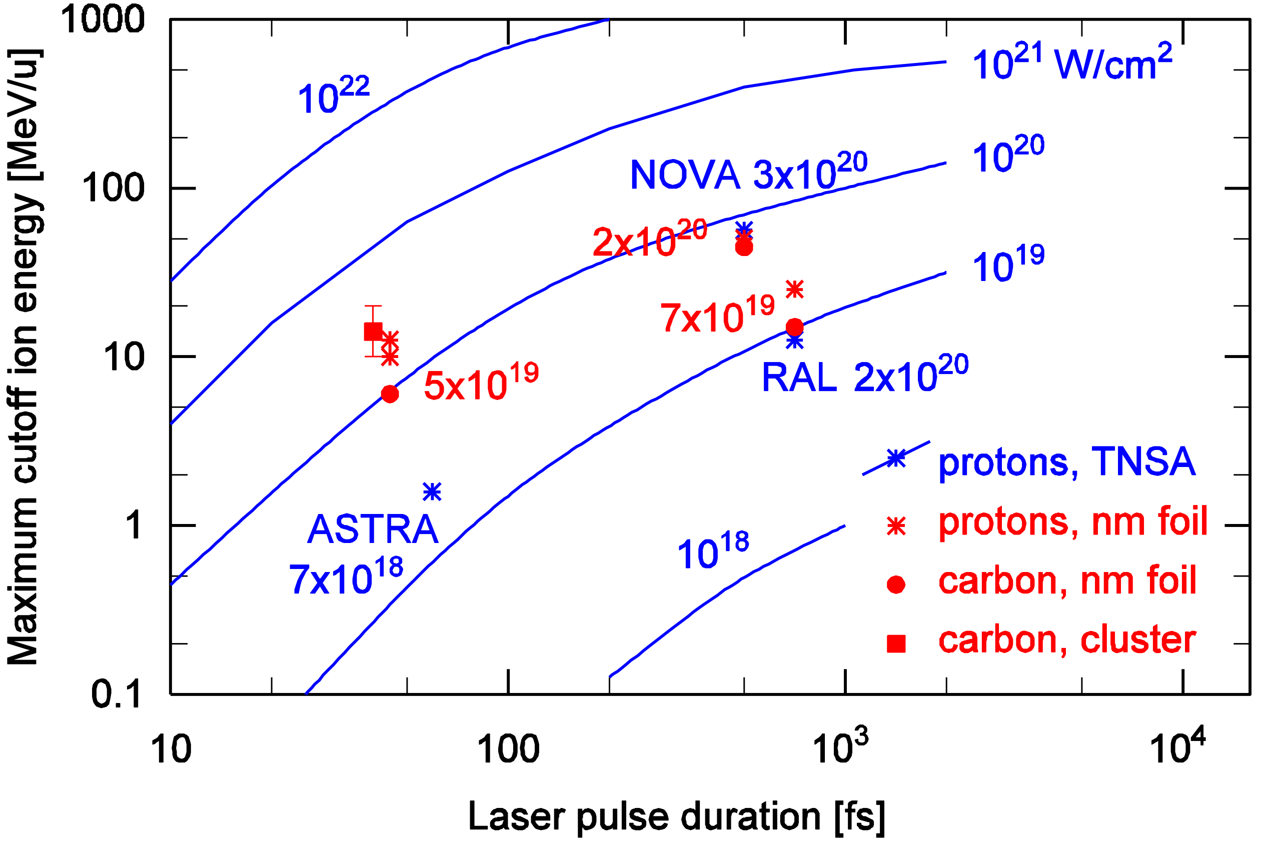

Tajima et al.
(2009)

Fig. 11. Maximum cutoff energies of ions given in MeV/u as a function of laser pulse duration. The energy gain by CAIL experiments is embedded with red dots in the predicted curves of **TNSA**. Note that in shorter pulses, energies by **CAIL** are more than an order of magnitude higher than TNSA.

Laser-driven protons in the past experiments

Daido et al. (2012)

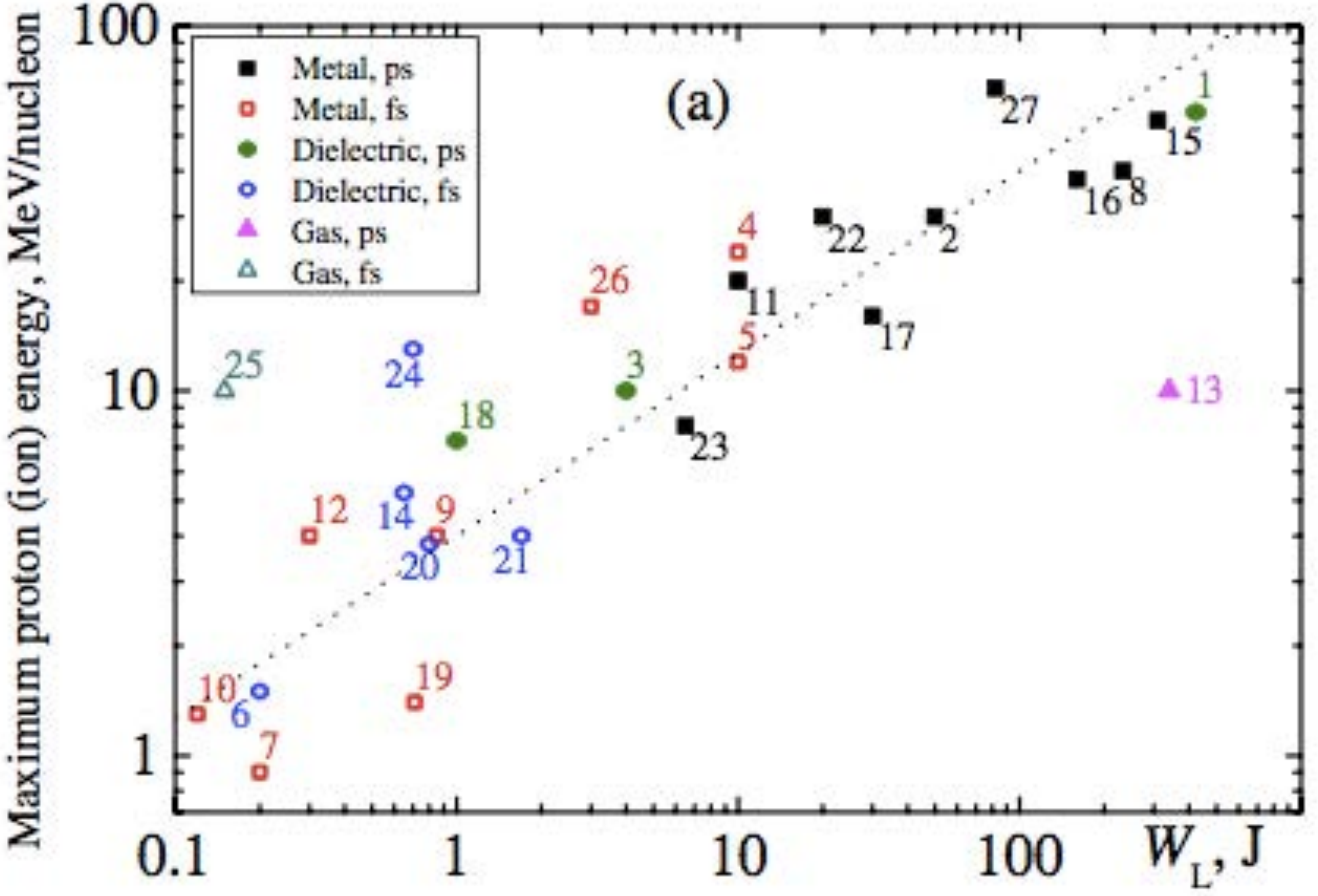

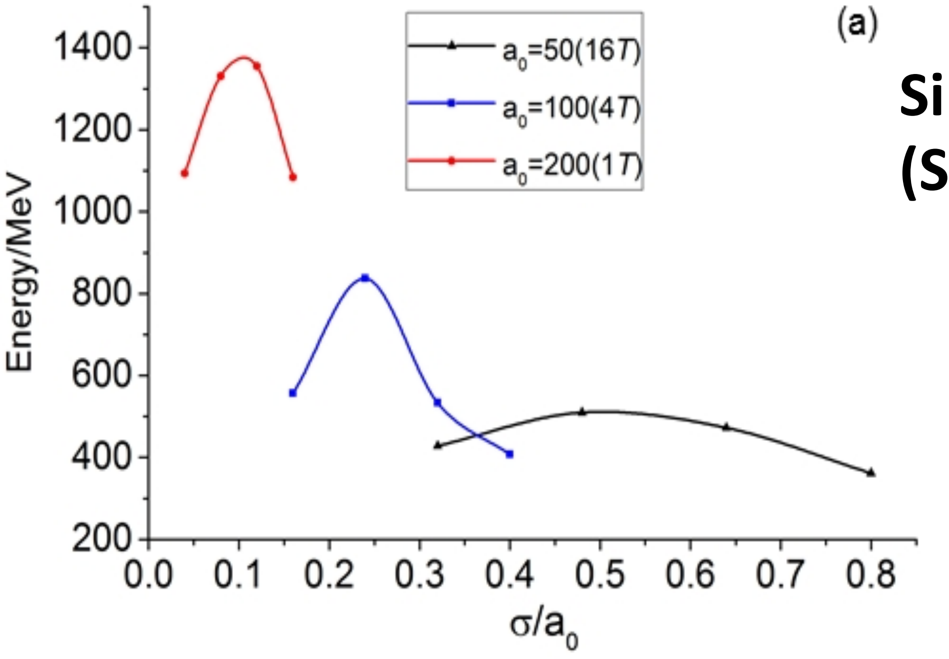

Single-Cycled Laser Acceleration (SCLA)

more coherent acceleration
under same laser energy: more energies proportional to a_0

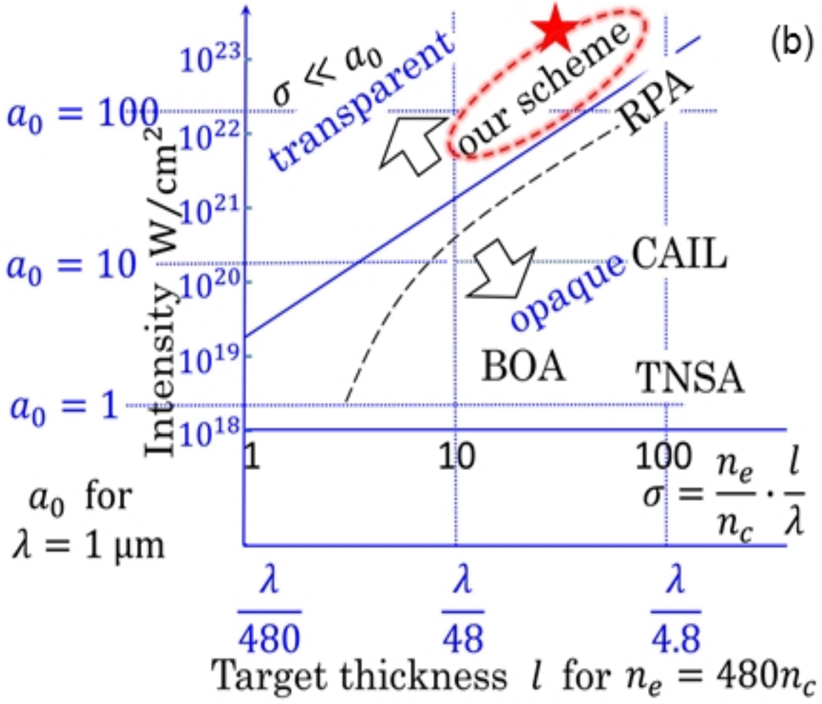

Domain map of various ion accelerations in a_0 and σ

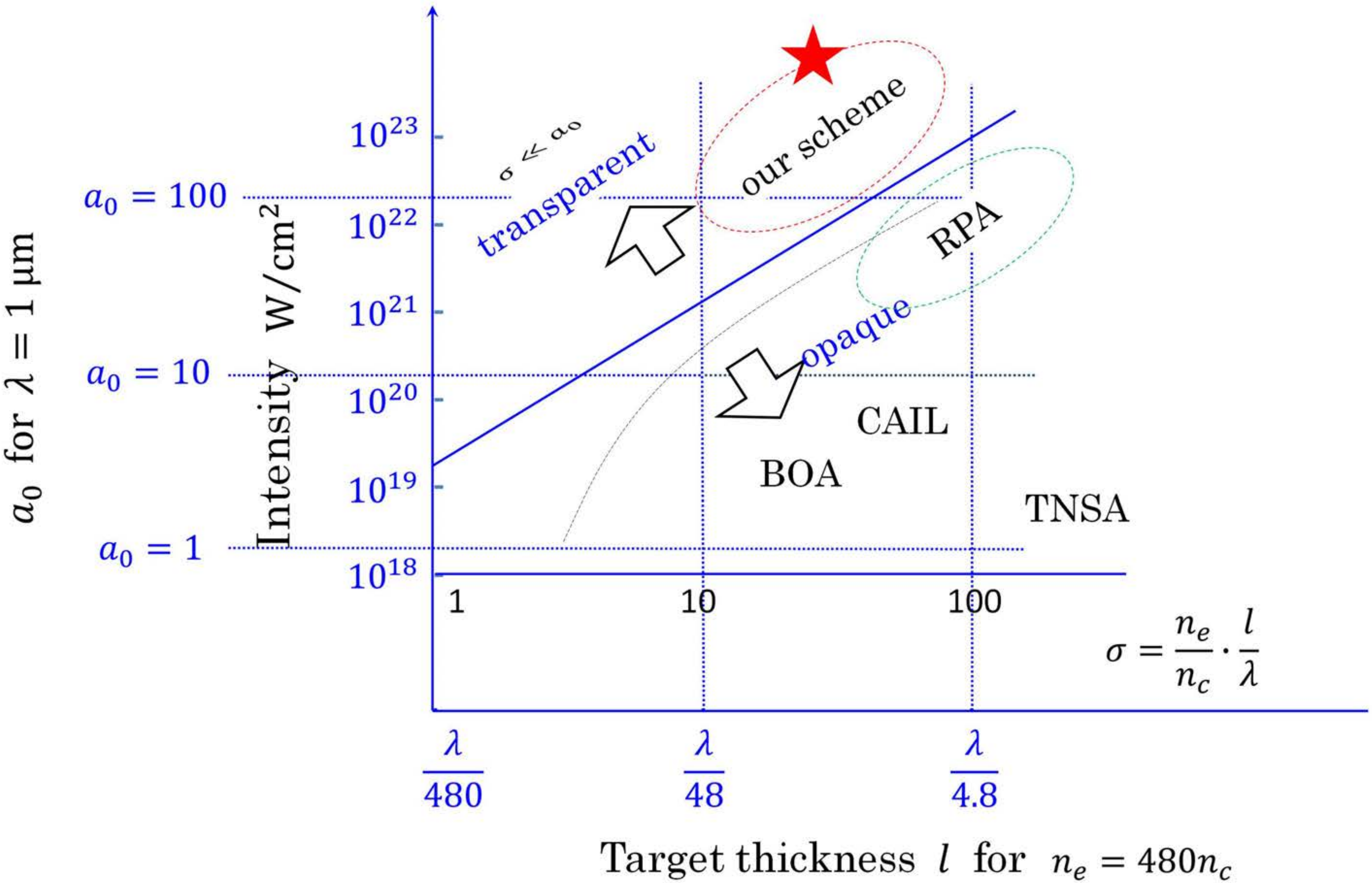

a_0 for $\lambda = 1\ \mu\text{m}$
Intensity W/cm^2
10^{23}
10^{22}
10^{21}
10^{20}
10^{19}
10^{18}
$a_0 = 100$
$a_0 = 10$
$a_0 = 1$
$\sigma \ll a_0$
transparent
opaque
our scheme
RPA
CAIL
BOA
TNSA
1
10
100
$\sigma = \frac{n_e}{n_c} \cdot \frac{l}{\lambda}$
$\frac{\lambda}{480}$
$\frac{\lambda}{48}$
$\frac{\lambda}{4.8}$
Target thickness l for $n_e = 480 n_c$

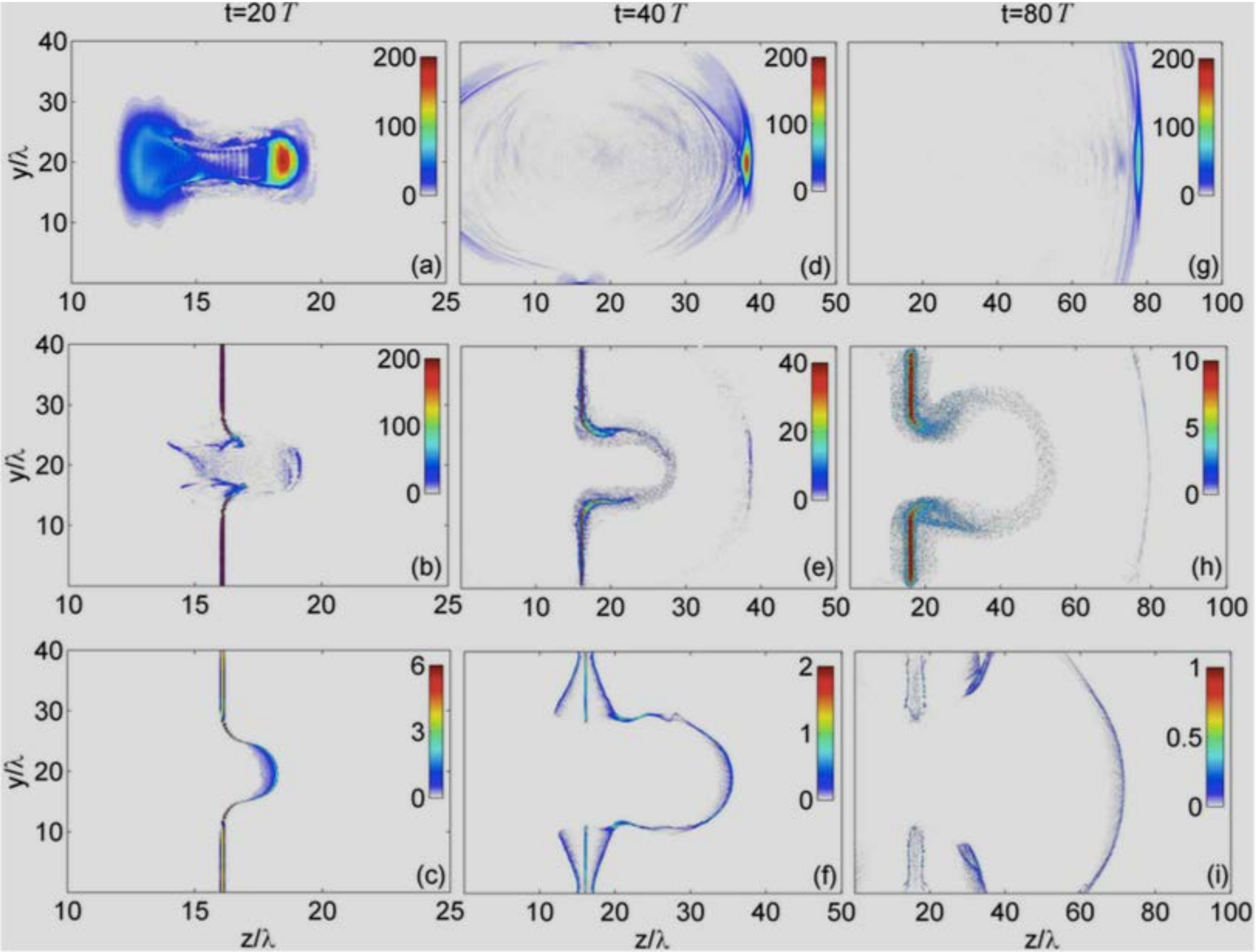
t=20 T
t=40 T
t=80 T
y/λ
z/λ
(a)
(b)
(c)
(d)
(e)
(f)
(g)
(h)
(i)
200
100
0
40
20
10
5
6
3
2
1
0.5
10
15
20
25
30
40
50
60
80
100

Thus when it counts to produce some radioactive isotopes, for example, that are not extremely short-lived but not too long-lived need to be produced at each needing hospital vicinity. A typical case may be the generation of **Cu^{64}, Cu^{67}** (the decay time of a few days) from **Zn^{64}, Zn^{67}** through the n-p processes [Kin, 2013; Kawabata, 2015].

Accelerated proton beams by laser as discussed in Chap. V can also play an important role to produce interesting **(p,n) processes**, which can also produce a host of isotopes of medical use. **These include O^{14} , Zr^{89} , Cu^{64}**. In these **(n,p), (p,n), (γ,p), and (p, γ) processes** the end products are chemically distinct from the start materials so that the separation of the products from the original is easier, as compared to such processes as (γ,n) and (n,γ), etc.

Table 1.6. Overview of alpha emitters used in nuclear medicine. Isotopes decaying mainly by beta-decay are shown in slanted letters.

Radio-nuclide	Half-life	Daughters	Half-life	Cumulative α/decay	E_α mean (MeV)	Range (µm)
Tb-149	4.1 h			0.17	3.97	25
Pb-212	*10.6 h*	Bi-212 Po-212	1.01 h 0.3 µs	1	7.74	65
Bi-212	1.01 h	Po-212	0.3 µs	1	7.74	65
Bi-213	*0.76 h*	Po-213	4 µs	1	8.34	75
At-211	7.2 h	Po-211	0.5 s	1	6.78	55
Ra-223	11.4 d	Rn-219 Po-215 *Pb-211* Bi-211	4 s 1.8 ms *0.6 h* 130 s	4	6.59	>50
Ra-224	3.66 d	Rn-220 Po-216 *Pb-212* Bi-212	56 s 0.15 s *10.6 h* 1.01 h	4	6.62	>50
Ac-225	10.0 d	Fr-221 At-217 *Bi-213* Po-213	294 s 32 ms *0.76 h* 4 µs	4	6.88	>50
Th-227	18.7 d	Ra-223 Rn-219 Po-215 *Pb-211* Bi-211	11.4 d 4 s 1.8 ms *0.6 h* 130 s	5	6.45	>50
U-230	20.8 d	Th-226 Ra-222 Rn-218 Po-214	0.51 h 38 s 35 ms 0.16 ms	5	6.71	>50

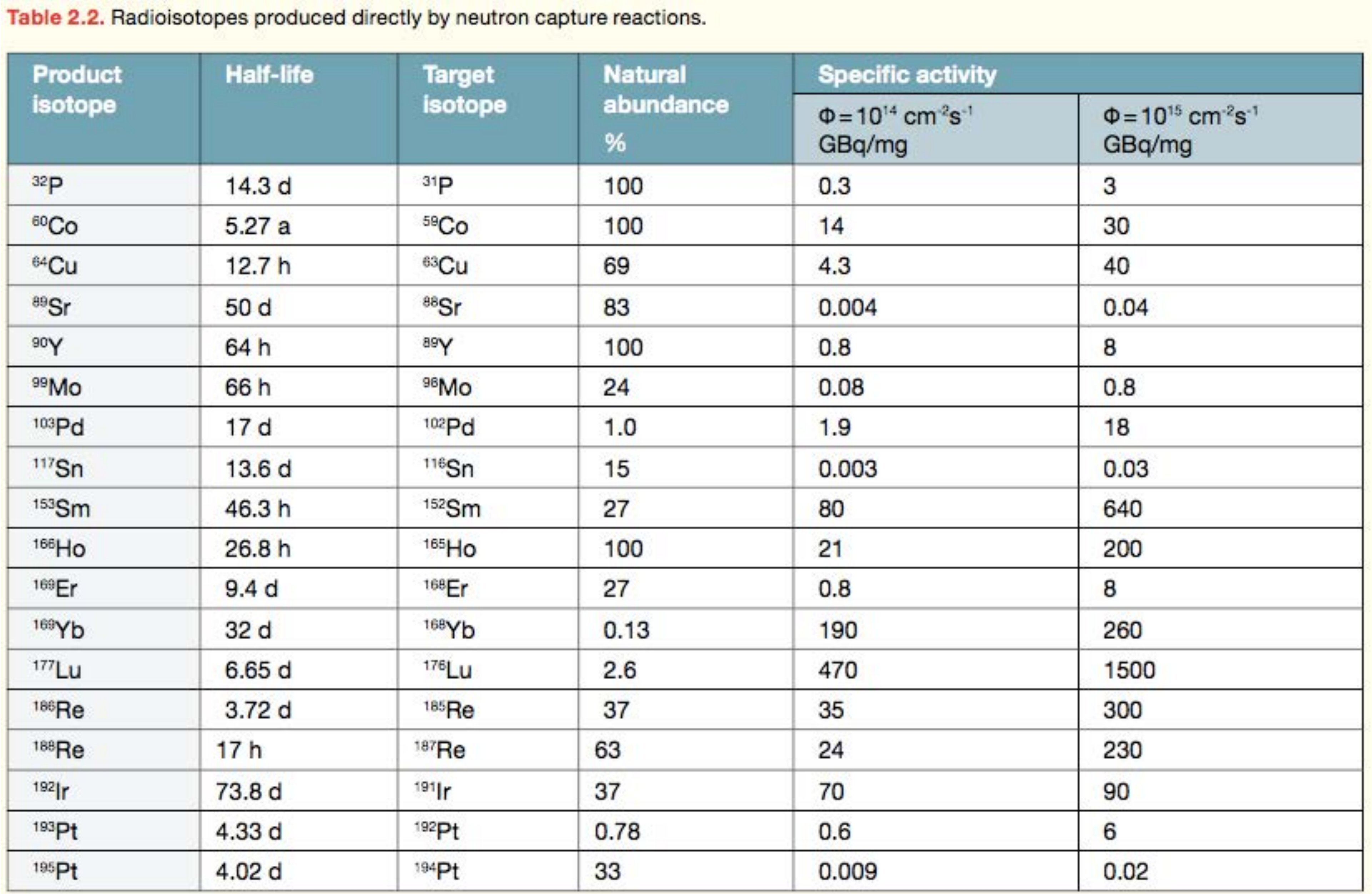

Table 2.2. Radioisotopes produced directly by neutron capture reactions.

Product isotope	Half-life	Target isotope	Natural abundance %	Specific activity	
				$\Phi = 10^{14}$ cm^{-2}s^{-1} GBq/mg	$\Phi = 10^{15}$ cm^{-2}s^{-1} GBq/mg
^{32}P	14.3 d	^{31}P	100	0.3	3
^{60}Co	5.27 a	^{59}Co	100	14	30
^{64}Cu	12.7 h	^{63}Cu	69	4.3	40
^{89}Sr	50 d	^{88}Sr	83	0.004	0.04
^{90}Y	64 h	^{89}Y	100	0.8	8
^{99}Mo	66 h	^{98}Mo	24	0.08	0.8
^{103}Pd	17 d	^{102}Pd	1.0	1.9	18
^{117}Sn	13.6 d	^{116}Sn	15	0.003	0.03
^{153}Sm	46.3 h	^{152}Sm	27	80	640
^{166}Ho	26.8 h	^{165}Ho	100	21	200
^{169}Er	9.4 d	^{168}Er	27	0.8	8
^{169}Yb	32 d	^{168}Yb	0.13	190	260
^{177}Lu	6.65 d	^{176}Lu	2.6	470	1500
^{186}Re	3.72 d	^{185}Re	37	35	300
^{188}Re	17 h	^{187}Re	63	24	230
^{192}Ir	73.8 d	^{191}Ir	37	70	90
^{193}Pt	4.33 d	^{192}Pt	0.78	0.6	6
^{195}Pt	4.02 d	^{194}Pt	33	0.009	0.02

Bracco e al, 2014

Radioisotopes

from intense, brilliant γ beams

(Habs, 2010)

Matched pairs: diagnostic and therapy isotope

frequently one of these isotopes was not available from
reactor or cyclotron

^{44}Sc/^{47}Sc; ^{61}Cu or ^{64}Cu/^{67}Cu; ^{86}Y/^{90}Y; ^{124}I/^{131}I

Auger cascades: 5–30 Auger electrons, low energy, 1μm range

Special bioconjugates transport emitter to DNA

no damage during transport or at cell membrane

Chain of α emitters:

^{225}Ra/^{225}Ac: 4 large LET α particles at the same place

Figure 2.16. Disassembled external gas target system filled with highly enriched ^{82}Kr for production of ^{81}Rb (top) and its position on an external beam line of the cyclotron U-120M (bottom); a similar target filled with ^{124}Xe is used for production of ^{123}I (Nuclear Physics Institute AS CR, v.v.i., Řež).

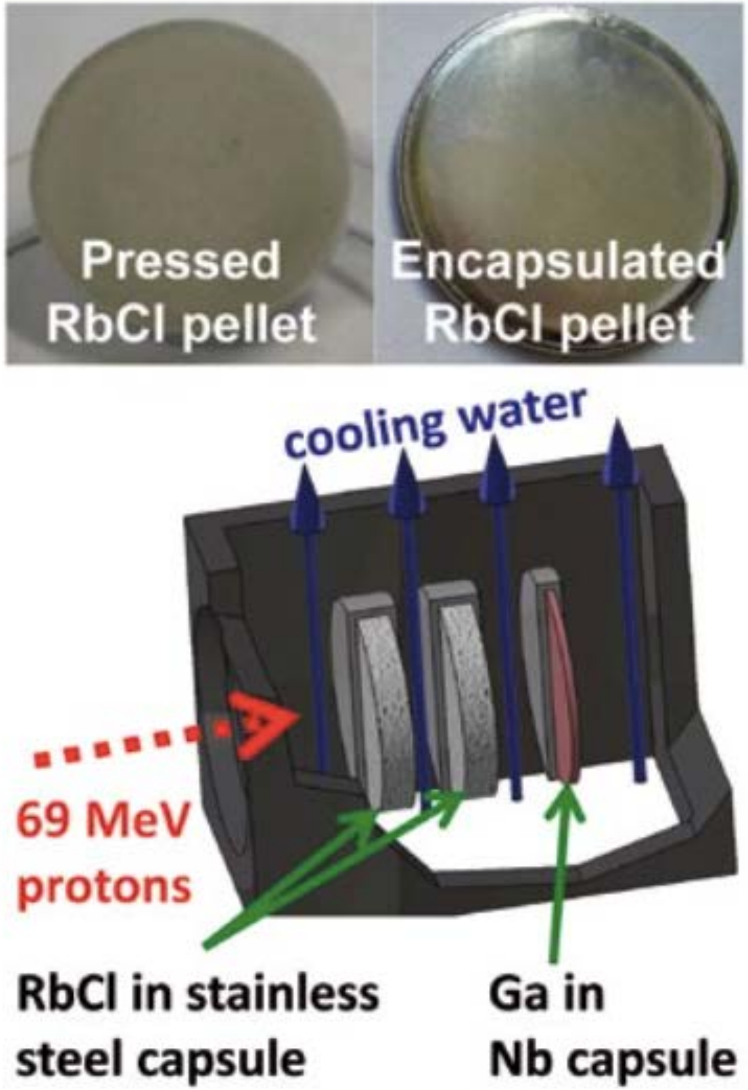

Figure 2.17. Example of an external perpendicular solid target system with 4π water cooling of two stainless steel capsules with RbCl targets for ^{82}Sr production and an additional niobium capsule with a Ga target for ^{68}Ge production (ARRONAX Nantes).

impurities are opened. With rising projectile energ

Bracco
2014

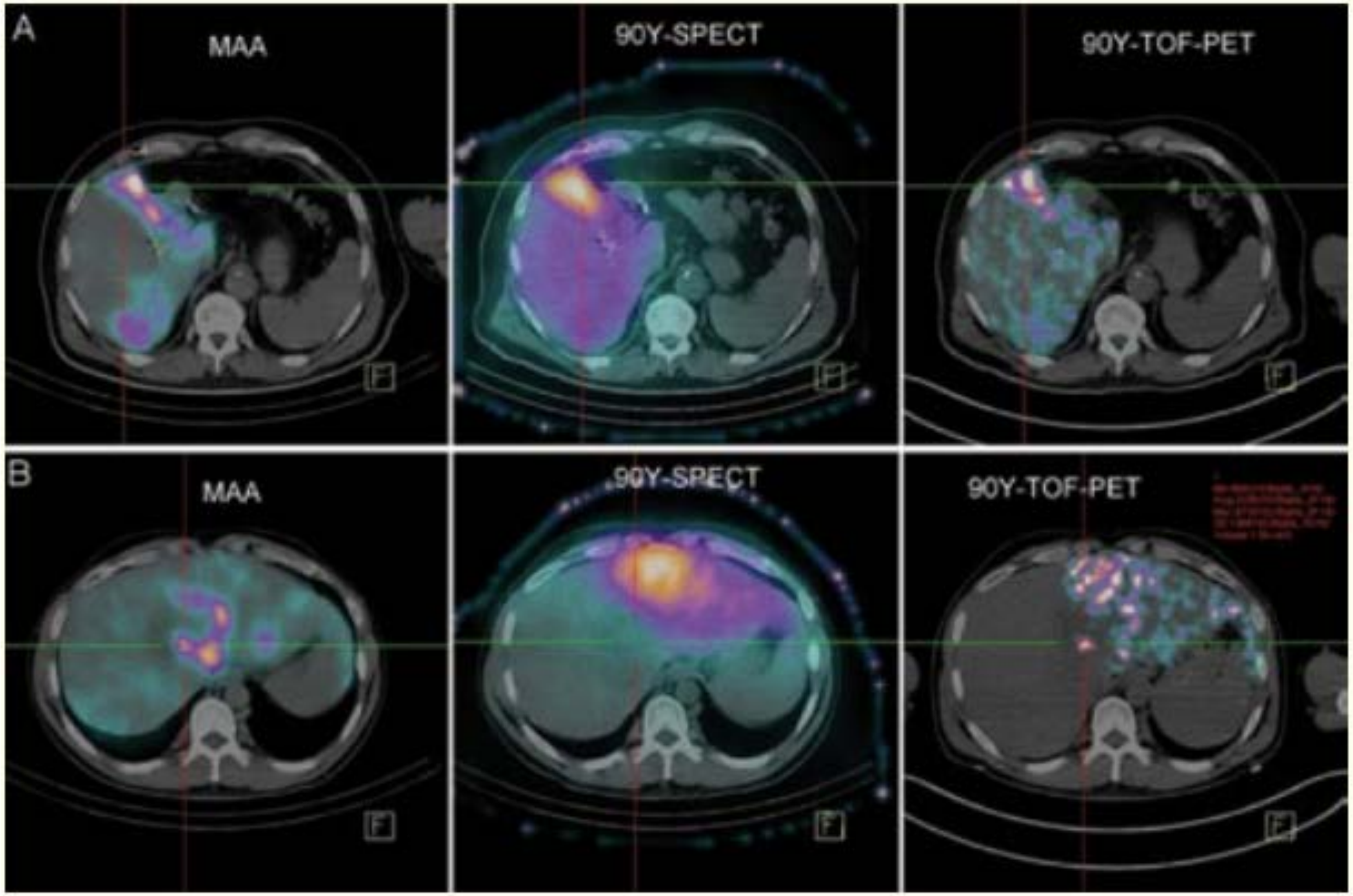

Figure 1.4. Different imaging techniques at the example of two patients (A on top, B on bottom) that were treated with ^{90}Y microspheres for radioembolisation of hepatic tumours. The left image shows ^{99m}Tc-MAA prior to treatment, the middle image ^{90}Y-Bremsstrahlung-SPECT and the right ^{90}Y-TOF-PET. The images were taken from Figure 7 of Th. Carlier *et al.*, *EJNMMI Research* 2013; **3**: 11 (Springer Open Access Licence, Creative Commons Attribution Licence).

M. Molls/ Japan Apr 09

Radiation

Homogeneous dose distribution

The tumor cell kill depends on intrinsic radiation sensitivity, DNA repair capacity, repopulation, oxygenation status etc.. However, the entire tumor can be irradiated homogeneously with that dose, which is necessary to kill all clonogenic tumor cells, even the most resistant ones.

Chemotherapy

Inhomogeneous dose distribution

The tumor cell kill depends on the transport of the substance to the clonogenic cells and molecular targets, DNA repair capacity, repopulation, pO2, pH, MDR, etc.. In macroscopic tumors not all the subvolumes of the tumor, clonogenic cells and relevant molecular targets are reached by those doses of the medical substance which are needed for cell kill.

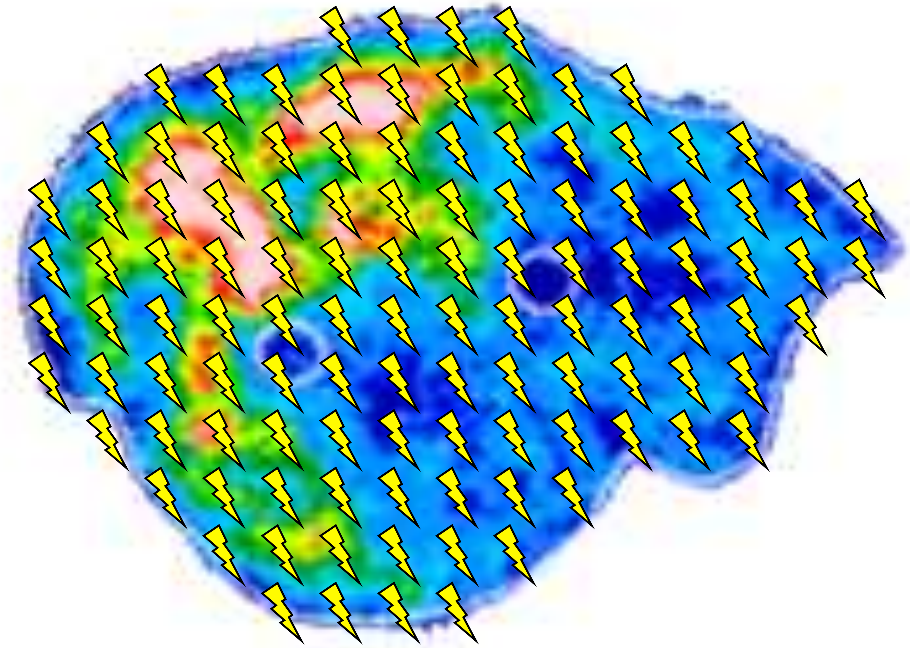

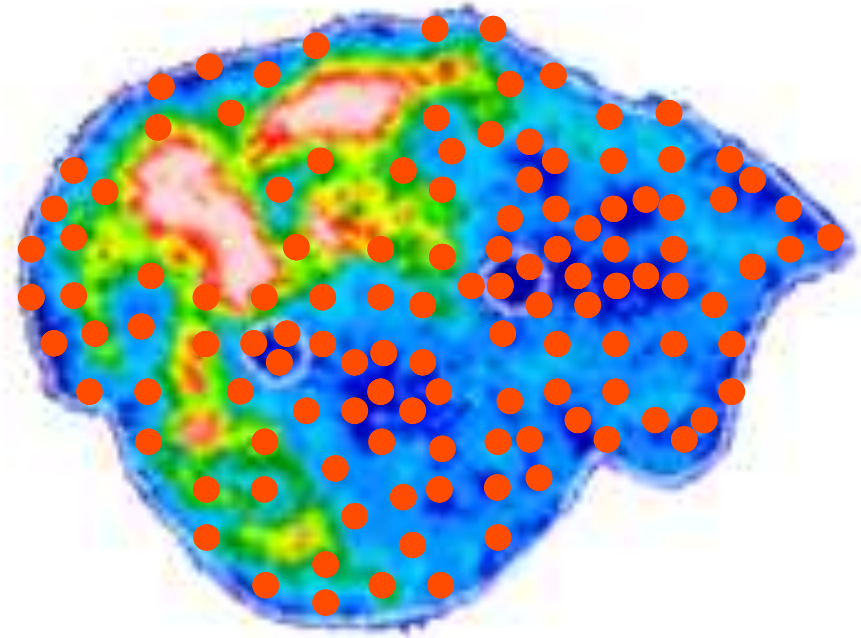

Conclusions

1. 10s MeV proton acceleration by laser: eminent possibility (compact, cheap laser method already exists)
2. transmutations by proton bema induced (p,n) processes relevant
3. transmulations by gamma-beam induced by (γ, p)
4. proton-induced neutrons: (n, p) processes
5. relatively short-lived radiative isotopes: good diagnostic markers; (under certain decays) good therapeutic killers
6. compatibility with the vector drug and physiology
7. impact on nuclear medicine and nuclear pharmacology
8. Convergence between medicine and laser critical: ELI-NP is critical to incubate this
9. ELI-NP: incubates the convergence of medicine and laser; launches the integration of science and entrepreneurial value creation
10. ELI-NP's immediate accomplishment
11. Strategy for ELI-NP future (a solution for the "2019 Problem")